**Table 6: Space-time power distribution $P_1(l, s, t \mid s^*, t^*)$ for the Rockaways ($s^* = 5$) on Day 33 ($t^* = 3$) with high risk (RR = 8. 48), where $t$ is a temporal length of detected cluster, and the raw all cells of which have zero powers of both tests is not shown. The mark "*" is the powers of accurate detection.**

(A) flexible ($K = 20$)

| | includes $s$ assumed areas | | | | | | | | | |
|---|---|---|---|---|---|---|---|---|---|---|
| | 1 | 2 | 3 | | 4 | | | 5 | | |
| length $l$ of areas | 31-$t = 3$ | 31-$t = 3$ | 31-$t = 3$ | 32-2 | 31-$t = 3$ | 32-2 | 33-1 | 31-$t = 3$ | 32-2 | 33-1 | total |
| 1 | 0 | | | | | | | | | | 0 |
| 2 | 0 | 0 | | | | | | | | | 6 |
| 3 | 0 | 2 | 6 | 0 | | | | | | | 22 |
| 4 | 0 | 0 | 20 | 0 | 181 | 1 | 0 | | | | 204 |
| 5 | 0 | 0 | 22 | 0 | 50 | 0 | 0 | *571 | 2 | 0 | 626 |
| 6 | 0 | 0 | 3 | 0 | 26 | 1 | 0 | 23 | 1 | 0 | 52 |
| 7 | 0 | 0 | 1 | 0 | 9 | 0 | 0 | 54 | 1 | 1 | 66 |
| 8 | 0 | 0 | 1 | 0 | 2 | 0 | 0 | 11 | 0 | 0 | 14 |
| 9 | 0 | 0 | 1 | 0 | 2 | 0 | 0 | 6 | 0 | 0 | 8 |
| 10 | 0 | 0 | 0 | 0 | 0 | 0 | 0 | 1 | 0 | 0 | 1 |
| 11 | 0 | 0 | 0 | 0 | 0 | 0 | 0 | 1 | 0 | 0 | 1 |
| 12 | 0 | 0 | 0 | 0 | 0 | 0 | 0 | 0 | 0 | 0 | 0 |
| 13 | 0 | 0 | 0 | 0 | 0 | 0 | 0 | 0 | 0 | 0 | 0 |
| 14 | 0 | 0 | 0 | 0 | 0 | 0 | 0 | 0 | 0 | 0 | 0 |
| 15 | 0 | 0 | 0 | 0 | 0 | 0 | 0 | 0 | 0 | 0 | 0 |
| 16 | 0 | 0 | 0 | 0 | 0 | 0 | 0 | 0 | 0 | 0 | 0 |
| 17 | 0 | 0 | 0 | 0 | 0 | 0 | 0 | 0 | 0 | 0 | 0 |
| 18 | 0 | 0 | 0 | 0 | 0 | 0 | 0 | 0 | 0 | 0 | 0 |
| 19 | 0 | 0 | 0 | 0 | 0 | 0 | 0 | 0 | 0 | 0 | 0 |
| 20 | 0 | 0 | 0 | 0 | 0 | 0 | 0 | 0 | 0 | 0 | 0 |
| total | 0 | 8 | 48 | 0 | 270 | 2 | 0 | 667 | 4 | 1 | 1000 |

(B) cylindrical ($K = 20$)

| | includes $s$ assumed areas | | | | | | | | | |
|---|---|---|---|---|---|---|---|---|---|---|
| length $l$ of areas | 1 | 2 | 3 | | 4 | | | 5 | | |
| | 31-$t = 3$ | 31-$t = 3$ | 31-$t = 3$ | 32-2 | 31-$t = 3$ | 32-2 | 33-1 | 31-$t = 3$ | 32-2 | 33-1 | total |
| 1 | 2 | | | | | | | | | | 2 |
| 2 | 0 | 8 | | | | | | | | | 8 |
| 3 | 0 | 0 | 52 | 1 | | | | | | | 53 |
| 4 | 0 | 0 | 0 | 0 | 876 | 6 | 1 | | | | 883 |
| 5 | 0 | 0 | 1 | 0 | 3 | 0 | 0 | *0 | 0 | 0 | 4 |
| 6 | 0 | 0 | 0 | 0 | 32 | 0 | 0 | 0 | 0 | 0 | 32 |
| 7 | 0 | 0 | 0 | 0 | 14 | 1 | 0 | 1 | 0 | 0 | 16 |
| 8 | 0 | 0 | 0 | 0 | 2 | 0 | 0 | 0 | 0 | 0 | 2 |
| 9 | 0 | 0 | 0 | 0 | 0 | 0 | 0 | 0 | 0 | 0 | 0 |
| 10 | 0 | 0 | 0 | 0 | 0 | 0 | 0 | 0 | 0 | 0 | 0 |
| 11 | 0 | 0 | 0 | 0 | 0 | 0 | 0 | 0 | 0 | 0 | 0 |
| 12 | 0 | 0 | 0 | 0 | 0 | 0 | 0 | 0 | 0 | 0 | 0 |
| 13 | 0 | 0 | 0 | 0 | 0 | 0 | 0 | 0 | 0 | 0 | 0 |
| 14 | 0 | 0 | 0 | 0 | 0 | 0 | 0 | 0 | 0 | 0 | 0 |
| 15 | 0 | 0 | 0 | 0 | 0 | 0 | 0 | 0 | 0 | 0 | 0 |
| 16 | 0 | 0 | 0 | 0 | 0 | 0 | 0 | 0 | 0 | 0 | 0 |
| 17 | 0 | 0 | 0 | 0 | 0 | 0 | 0 | 0 | 0 | 0 | 0 |
| 18 | 0 | 0 | 0 | 0 | 0 | 0 | 0 | 0 | 0 | 0 | 0 |
| 19 | 0 | 0 | 0 | 0 | 0 | 0 | 0 | 0 | 0 | 0 | 0 |
| 20 | 0 | 0 | 0 | 0 | 0 | 0 | 0 | 0 | 0 | 0 | 0 |
| total | 2 | 8 | 53 | 1 | 927 | 7 | 1 | 1 | 0 | 0 | 1000 |

The extended power is based on the bivariate distribution $P_0(l, s \mid s^*)$ and penalties introduced for the FPs and FNs of the geographical detection as

$$I(w^-, w^+) = \sum_{l\geq 1}\sum_{s\geq 0} W(l, s; w^-, w^+) P_0(l, s \mid s^*) \quad (8)$$

where $W(l, s; w^-, w^+)$ is a weight function such that

$$W(l, s; w^-, w^+) = \begin{cases} \sqrt{\left(1 - \min\{w^-(s^* - s), 1\}\right)\left(1 - \min\{w^+(l - s), 1\}\right)}, & (s \leq l; 0 \leq s \leq s^*, 1 \leq l), \\ 0, & (\text{otherwise}) \end{cases} \quad (9)$$

and $w^-$ and $w^+$ are the predefined penalties for the FNs and FPs (per region), respectively. This power includes the following three special powers:

1. The standard power as $I(0, 0)$.

2. The power to detect the geographical true cluster accurately as $I(1, 1)$.

3. The power for which the MLC includes all the regions within the true cluster as $I(1, 0)$.

Takahashi and Tango [26] also proposed the profile of the extended power as

$$Q(r \mid s^*) = I(1/s^*, r/s^*), \quad (0 \leq r \leq 1) \quad (10)$$

where $r = w^+/w^-$ with $w^- = 1/s^*$, because it is difficult to set the value of $w^-$ and $w^+$ in advance. Figure 3 shows the plots of the profile $Q(r \mid s^*)$ against $r\,(0 \leq r \leq 1)$ for flexible and cylindrical scan statistics applied to (a) the cluster A5 and (b) the Rockaways, both on Day 33 with high risk, based upon Tables 5 and 6. Figure 3(a) shows the flexible scan statistic has higher extended power when $r = 0$ i.e. penalties for the FP $w^+ = 0$, $I(1/5, 0) = 0.978$ for the flexible and 0.954 for the cylindrical, while the extended power of cylindrical scan statistic is higher for large $r$, as $I(1/5, 1/5) = 0.765$ for the flexible and 0.862 for the cylindrical. On the other hand, Figure 3(b) shows the flexible scan statistic is more uniformly powerful than the cylindrical one for the Rockaways cluster, $I(1/5, 0) = 0.958$ and $I(1/5, 1/5) = 0.913$ for the flexible, and $I(1/5, 0) = 0.885$ and $I(1/5, 1/5) = 0.872$ for the cylindrical, respectively.

### *Sensitivity and positive predictive value*

As other measures of accuracy of cluster detection tests, we shall consider sensitivity and positive predictive value [27,28]. These measures can be defined in terms of either *the number of regions* or *the population*. First, we define *sensitivity* of cluster detection tests as the probability of detecting the regions that actually constitute the cluster, i.e, proportion of the number of regions correctly detected from the true cluster, $s/s^*$. We shall present the expected value:

$$TP_1 = E\left[\frac{S}{s^*}\right] = \sum_{s=0}^{s^*} \frac{s}{s^*} P_0(+, s \mid s^*). \quad (11)$$

*Positive predictive value* (PPV) of cluster detection tests is defined in a similar manner as the proportion of the number of true regions in the detected cluster, i.e, $s/l$ under $l > 0$, and the expected value is presented:

$$PP_1 = E\left[\frac{S}{L}\middle| L>0\right] = \sum_{l\geq 1}\sum_{s\geq 0} \frac{s}{l} \frac{P_0(l, s \mid s^*)}{P_0(+, + \mid s^*)} \quad (12)$$

Based upon the population, we can define the following sensitivity $TP_2$ and positive predictive value $PP_2$:

$$TP_2 = \frac{E(\text{Total population of the detected } S \text{ true regions})}{\text{Total population of the } s^* \text{ reigons of true cluster}} \quad (13)$$

$$PP_2 = E\left(\frac{\text{Total population of } S \text{ true regions}}{\text{Total population of } L \text{ detected regions}}\middle| L>0\right) \quad (14)$$

All these summary measures are better the larger they are with 100 being the optimal.

Table 7 shows the sensitivity and PPV of the flexible and cylindrical space-time scan statistics for each cluster with a high relative risk. For cluster A, the cylindrical scan statistic has higher PPV and higher sensitivity than the flexible one. For cluster A5 and the cylindrical has higher PPV on all days and higher sensitivity on day 31, but the flexible scan statistic has higher sensitivity on days 32 and 33. The same is true for the Rockaway cluster. For the Hudson River cluster, the flexible scan statistic has higher PPV than the cylindrical. The flexible scan has higher sensitivity than for the cylindrical with the same upper constant $K = 20$ on the number of regions in the detected cluster, but lower sensitivity compared to the cylindrical scan with a 50% upper limit on the cluster size. Note though, that this difference in sensitivity is less than the difference in PPV that goes the other way.

## Conclusion

In this paper, we have proposed a flexible space-time scan statistic to detect arbitrarily shaped disease outbreaks. We have also presented a tri-variate power distribution which is useful for evaluating the performance of cluster detection tests, informing us about the spatial and temporal

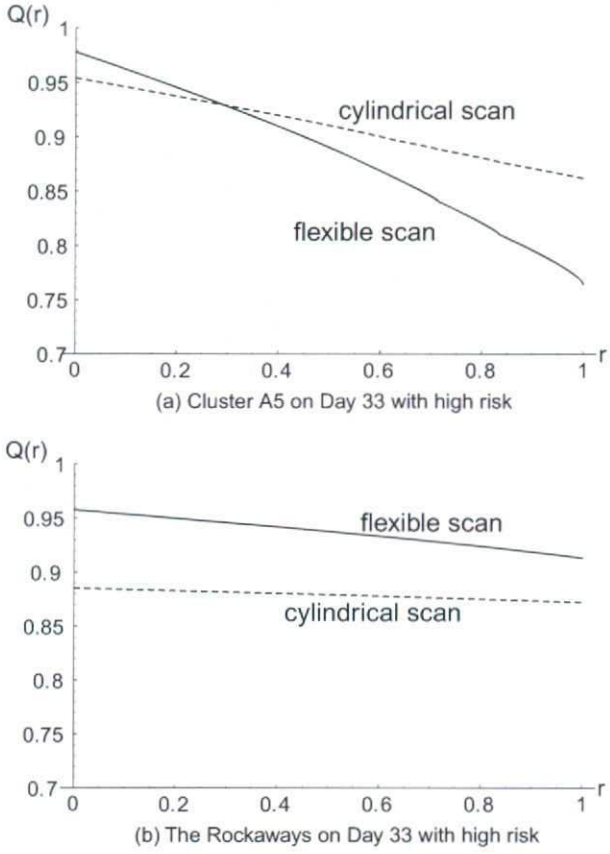


**Figure 3**
**Profile of the extended power $Q(r \mid s^*)$ for flexible and cylindrical scan statistics applied to the cluster (a) Cluster A5, and (b) The Rockaways.**

accuracy of the detected clusters in addition to the standard statistical power.

For the benchmark data evaluated in this paper, the cylindrical scan statistic performs better for the small single zip-code cluster, although by the third day of the outbreak both methods are almost perfect. For the small irregular shaped clusters, A5 and Rockaways, the cylindrical performs better on the first day of the outbreak, but as more data accumulates, the flexible scan statistic has certain advantages in determining the precise size and shape of the outbreak. For the large and narrow Hudson River cluster, the flexible scan statistic performs better than the cylindrical one, with slightly higher standard power, much higher PPV and slightly higher or lower sensitivity depending on the type of cylindrical method used. Results may be different for other types of regular and irregularly shaped disease outbreaks, but the four examples used in this paper gives some sense of the proposed methods performance.

For early detection, timeliness is much more important than geographical accuracy. When monitoring an occurring outbreak, on the other hand, geographical accuracy becomes critical and is then the key objective since we already know the outbreak is there. Our results suggest that we may use both the cylindrical and flexible scan statistic for disease outbreak detection, but for different purposes. Specifically, for detecting new outbreak that, one may want to use the cylindrical scan statistic. That is especially if we expect the outbreak to start locally, within a reasonably small and compact area containing only a few ZIP-codes. On the other hand, once the outbreak has spread to a larger area, and we want to monitor that spread, one may want to use the flexible scan statistic, with its ability to accuratly determine the precise geographical extent of irregular shaped outbreaks. This is especially true ones the outbreak has left its local area of origin.

To evaluate the performance of space-time scan statistic, we applied the extended power for purely spatial cluster detection test (8), which is defined as the weighted sum of the bivariate power distribution wherein the weight is given by the geometric mean of (1-penalty for the false negatives) and (1-penalty for the false positives), including the standard power as a special case. Also we applied the profile $Q(r / s^*)$ proposed by Takahashi and Tango [26]. This plot gave us a detailed description regarding power of cluster detection tests. Needless to say, it is possible to extend it to space-time version if we could consider the penalties for temporal false negatives and false positives, but we leave this problem for future work. Also, for the profile of the extended power, we chose to use a fixed cost of $w = 1/s^*$ for false negatives and a smaller or equal cost for false positives. For more general situations, we could plot the full bivariate extended power function on the unit square.

Similarly to the flexible spatial scan statistic in the purely spatial situation, the flexible space-time scan statistics proposed in this paper has a limitation of cluster size, because of the limitation of the speed of computation. The proposed scan statistic works well for small to moderate sized clusters. Although we set the maximum length of the geographical window to $K = 20$, this is not large enough to detect the 20 ZIP codes of the Hudson River cluster accurately because this cluster is too long to be the subset of the 20-th nearest neighbors of any region. Computation time depends on the size of the data set and $K$. Indeed, for the August 11 analysis of respiratory syndrome data in Massachusetts, with 385 ZIP codes, a maximum temporal length of $T = 7$ days, a maximum spatial size of $K = 20$, and

**Table 7: Sensitivity and positive predictive value (PPV) of the flexible and cylindrical space-time scan statistics.**

| | | | zip codes | | population | |
|---|---|---|---|---|---|---|
| | | traditional power | sensitivity (%) | PPV (%) | sensitivity (%) | PPV (%) |
| **Cluster A**; $s^* = 1$; high risk | | | | | | |
| Day 31 | flexible ($K = 20$) | | | | | |
| | cylindrical ($K = 20$) | 0.860 | 85.30 | 89.45 | 85.30 | 91.50 |
| | cylindrical (50% pop) | 0.862 | 85.90 | 88.79 | 85.90 | 90.84 |
| Day 32 | flexible ($K = 20$) | 0.988 | 98.80 | 84.50 | 98.80 | 87.80 |
| | cylindrical ($K = 20$) | 0.996 | 99.50 | 97.44 | 99.50 | 98.18 |
| | cylindrical (50% pop) | 0.996 | 99.50 | 97.33 | 99.50 | 98.08 |
| Day 33 | flexible ($K = 20$) | 0.999 | 99.90 | 96.27 | 99.90 | 97.32 |
| | cylindrical ($K = 20$) | 0.999 | 99.90 | 99.48 | 99.90 | 99.65 |
| | cylindrical (50% pop) | 0.999 | 99.90 | 99.48 | 99.90 | 99.65 |
| **Cluster A5**; $s^* = 5$; high risk | | | | | | |
| Day 31 | flexible ($K = 20$) | 0.797 | 66.08 | 55.93 | 67.29 | 63.00 |
| | cylindrical ($K = 20$) | 0.850 | 69.62 | 80.35 | 71.65 | 84.21 |
| | cylindrical (50% pop) | 0.847 | 70.62 | 78.17 | 71.62 | 82.02 |
| Day 32 | flexible ($K = 20$) | 0.994 | 92.22 | 70.17 | 92.94 | 76.73 |
| | cylindrical ($K = 20$) | 0.996 | 88.78 | 85.14 | 90.86 | 89.41 |
| | cylindrical (50% pop) | 0.996 | 88.96 | 84.81 | 91.05 | 89.11 |
| Day 33 | flexible ($K = 20$) | 1.000 | 95.88 | 80.02 | 96.64 | 85.25 |
| | cylindrical ($K = 20$) | 1.000 | 91.42 | 87.32 | 93.66 | 91.67 |
| | cylindrical (50% pop) | 1.000 | 91.42 | 87.30 | 93.66 | 91.65 |
| **The Rockaways**; $s^* = 5$; high risk | | | | | | |
| Day 31 | flexible ($K = 20$) | 0.769 | 60.68 | 72.09 | 69.04 | 73.58 |
| | cylindrical ($K = 20$) | 0.855 | 62.32 | 91.63 | 74.45 | 91.76 |
| | cylindrical (50% pop) | 0.840 | 61.40 | 91.04 | 73.65 | 91.15 |
| Day 32 | flexible ($K = 20$) | 0.992 | 86.76 | 87.36 | 94.17 | 89.86 |
| | cylindrical ($K = 20$) | 0.997 | 77.00 | 96.84 | 92.75 | 97.46 |
| | cylindrical (50% pop) | 0.997 | 77.00 | 96.84 | 92.75 | 97.46 |
| Day 33 | flexible ($K = 20$) | 1.000 | 92.16 | 93.81 | 97.15 | 95.97 |
| | cylindrical ($K = 20$) | 1.000 | 78.50 | 98.06 | 94.51 | 98.59 |
| | cylindrical (50% pop) | 1.000 | 78.50 | 98.06 | 94.51 | 98.59 |
| **Hudson River**, $s^* = 20$; high risk | | | | | | |
| Day 31 | flexible ($K = 20$) | 0.656 | 20.07 | 64.99 | 26.00 | 69.72 |
| | cylindrical ($K = 20$) | 0.597 | 14.23 | 61.10 | 18.16 | 65.18 |
| | cylindrical (50% pop) | 0.632 | 26.15 | 50.70 | 31.26 | 53.71 |
| Day 32 | flexible ($K = 20$) | 0.964 | 32.17 | 73.59 | 41.81 | 78.36 |
| | cylindrical ($K = 20$) | 0.933 | 24.13 | 61.55 | 31.58 | 66.69 |
| | cylindrical (50% pop) | 0.949 | 42.90 | 50.27 | 51.50 | 53.96 |
| Day 33 | flexible ($K = 20$) | 0.998 | 34.91 | 79.39 | 46.27 | 84.17 |
| | cylindrical ($K = 20$) | 0.994 | 27.23 | 60.56 | 36.75 | 66.20 |
| | cylindrical (50% pop) | 0.995 | 48.14 | 47.34 | 58.54 | 51.34 |

with 999 Monte Carlo replications, the flexible space-time scan statistic took 87.7 minutes to run on a 3.06-GHz Pentium 4 computer, while the cylindrical space-time scan statistic took only 9.8 minutes.

A limitation of length may also prevent the analysis to present large clusters of unlikely and very peculiar shapes. These undesirable properties produced by maximum likelihood ratio might suggest the use of different criterion for model selection, including some penalized likelihood [20,29]. Also, for larger cluster seizes, the method is not practically feasible and a more efficient algorithm is needed.

In this paper, we considered the *right* cylinder or *right* prism of the cluster model, as an expansion of the cylindrical space-time scan statistic for a prospective disease surveillance by Kulldorff [10]. This does not allow the scanning window to adjust itself as the disease outbreak grows or shrinks geographically over time. Recently, Iyengar has suggested using a *square pyramid shape* window

which can model either growth (or shrinkage) and movement of the disease cluster [30]. For the proposed flexible space-time scan statistic, if we could consider the flexibility in both space and time, that is, evaluating all connected subsets within a cylinder instead of $\mathcal{W}$ in (4), we can detect more arbitrarily shaped clusters in space-time. For such an expansion, an efficient computational algorithm will be needed for the scanning process, as well as a more sophisticated mechanism for the interpretation of such complicatedly shaped clusters. The implementation and importance of such methods for disease surveillance and monitoring, is an issue for future research.

## Authors' contributions

KT, MK and TT developed the statistical methodology and designed the study. KT, MK and KY analyzed and interpreted the syndromic surveillance data. KT programmed the methods, did the power calculations and wrote the first draft of the manuscript. All authors participated in the interpretation of the results, revised the manuscript, and approved the final version.

## Acknowledgements

The authors thank Allyson Abrams for comments concerning the syndromic surveillance data from Massachusetts, and Dr. Tetsuji Yokoyama for advice about C++ programming.

This research was partly founded by a Modeling Infectious Disease Agent Study (MIDAS) grant (No. U01GM076672) from the National Institute of General Medical Science, National Institutes of Health, USA, and a scientific grant (No. H16-Kenkou-039) from the Ministry of Health, Labour and Welfare, Japan.

## References

1. Heffernan R, Mostashari F, Das D, Karpati A, Kulldorff M, Weiss D: **Syndromic surveillance in public health practice, New York City.** *Emerging Infectious Diseases* 2004, **10**:858-864.
2. Lombardo J, Burkom H, Elbert E, Magruder S, Lewis SH, Loschen W, Sari J, Sniegoski C, Wojcik R, Pavlin J: **A systems overview of the electronic surveillance system for the early notification of community-based epidemics (ESSENCE II).** *Journal of Urban Health* 2003, **80(2 suppl.1)**:i32-i42.
3. Lazarus R, Kleinman K, Dashevsky I, Adams C, Kludt P, DeMaria A, Platt R: **Use of automated ambulatory-care encounter records for detection of acute illness clusters, including potential bioterrorism events.** *Emerg Infect Dis* 2002, **8(8)**:753-760.
4. Platt R, Bocchino C, Caldwell B, Harmon R, Kleinman K, Lazarus R, Nelson AF, Nordin JD, Ritzwoller P: **Syndromic surveillance using minimum transfer of identifiable data: the example of the National Bioterrorism Syndromic Surveilance Demonstration Program.** *Journal of Urban Health* 2003, **80(2 suppl.1)**:i25-i31.
5. Sonesson C, Bock D: **A review and discussion of prospective statistical surveillance in public health.** *Journal of the Royal Statistical Society, Series A* 2003, **166**:5-21.
6. Lawson AB, Kleinman K, Eds: *Spatial & Syndromic Surveillance for Public Health* Chichester: Wiley; 2005.
7. Naus J, Wallenstein S: **Temporal surveillance using scan statistics.** *Statistics in Medicine* 2006, **25**:311-324.
8. Kulldorff M: **A spatial scan statistic.** *Communications in Statistics – Theory and Methods* 1997, **26**:1481-1496.
9. Rogerson PA, Yamada I: **Monitoring change in spatial patterns of disease: comparing univariate and multivariate cumulative sum approaches.** *Statistics in Medicine* 2004, **23**:2195-2214.
10. Kulldorff M: **Prospective time periodic geographical disease surveillance using a scan statistic.** *Journal of the Royal Statistical Society, Series A* 2001, **164**:61-72.
11. Kulldorff M, Heffernan R, Hartman J, Assunção R, Mostashari F: **A space-time permutation scan statistic for disease outbreak detection.** *PLoS Medicine* 2005, **2(3)**:e59.
12. Lawson AB, Biggeri A, Böhning D, Lesaffre E, Viel JF, Bertollini R, Eds: *Disease Mapping and Risk Assessment for Public Health* New York: Wiley; 1999.
13. Lawson AB: *Statistical Methods in Spatial Epidemiology* 2nd edition. Chichester: Wiley; 2006.
14. Kulldorff M, Information Management Services, Inc: **SaTScan version 7.0: software for the spatial and space-time scan statistics.** 2007 [http://www.satscan.org/].
15. Kulldorff M: **Scan statistics for geographical disease surveillance: an overview.** In *Spatial & Syndromic Surveillance for Public Health* 2nd edition. Edited by: Lawson AB, Kleinman K. Chichester: Wiley; 2005:115-131.
16. Tango T, Takahashi K: **A flexibly shaped spatial scan statistic for detecting clusters.** *International Journal of Health Geographics* 2005, **4(11)**:.
17. Duczmal L, Assunção R: **A simulated annealing strategy for the detection of arbitrarily shaped spatial clusters.** *Computational Statistics & Data Analysis* 2004, **45**:269-286.
18. Patil GP, Taillie C: **Upper level set scan statistic for detecting arbitrarily shaped hotspots.** *Environmental and Ecological Statistics* 2004, **11**:183-197.
19. Assunção R, Costa M, Tavares A, Ferreira S: **Fast detection of arbitrarily shaped disease clusters.** *Statistics in Medicine* 2006, **25**:723-742.
20. Kulldorff M, Huang L, Pickle L, Duczmal L: **An elliptic spatial scan statistic.** *Statistics in Medicine* 2006, **25**:3929-3943.
21. Takahashi K, Yokoyama T, Tango T: **FleXScan version 2.0: Software for the Flexible Spatial Scan Statistic.** *Japan* 2007 [http://www.niph.go.jp/soshiki/gijutsu/index_e.html].
22. Kulldorff M, Zhang Z, Hartman J, Heffernan R, Huang L, Mostashari F: **Benchmark data and power calculations for evaluating disease outbreak detection methods.** *Morbidity and Mortality Weekly Report* 2004, **53(Supplement 1)**:144-151.
23. Dwass M: **Modified randomization tests for nonparametric hypotheses.** *The Annals of Mathematical Statistics* 1957, **28**:181-187.
24. Lazarus R, Kleinman K, Dashevsky I, DeMaria A, Platt R: **Using automated medical records for rapid identification of illness syndromes (syndromic surveillance): the example of lower respiratory infection.** *BMC Public Health* 2001, **1**:9.
25. Kleinman K, Lazarus R, Platt R: **A generalized linear mixed models approach for detecting incident clusters of disease in small areas, with an application to biological terrorism.** *American Journal of Epidemiology* 2004, **159**:217-224.
26. Takahashi K, Tango T: **An extended power of cluster detection tests.** *Statistics in Medicine* 2006, **25**:841-852.
27. Forsberg L, Bonetti M, Jeffery C, Ozonoff A, Pagano M: **Distance-based methods for spatial and spatio-temporal surveillance.** In *Spatial & Syndromic Surveillance for Public Health* 2nd edition. Edited by: Lawson AB, Kleinman K. Chichester: Wiley; 2005:115-131.
28. Huang L, Kulldorff M, Gregorio D: **A spatial scan statistic for survival data.** *Biometrics* 2007, **63**:109-118.
29. Duczmal L, Kulldorff M, Huang L: **Evaluation of spatial scan statistics for irregularly shaped clusters.** *Journal of Computational and Graphical Statistics* 2006, **15(2)**:428-442.
30. Iyengar VS: **Space-time clusters with flexible shapes.** *Morbidity and Mortality Weekly Report* 2005, **54(Supplement)**:71-76.

Japanese Journal of Biometrics Vol. 29, No. 2, 75–95 (2008)

Original Article

# A Spatial Scan Statistic with a Restricted Likelihood Ratio

Toshiro Tango

Department of Technology Assessment and Biostatistics
National Institute of Public Health,
3-6 Minami 2 chome, Wako, Saitama, 351-0197, Japan
e-mail:tango@niph.go.jp

Kulldorff (1997) developed a circular spatial scan statistic for identifying the most likely cluster of disease that maximizes the likelihood ratio and his software SaTScan has been widely used for geographical disease cluster detection and disease surveillance. To detect non-circular clusters which cannot be detected by Kulldorff's circular spatial scan statistic, several non-circular spatial scan statistics have been proposed. However, it does not seem to be well recognized that these spatial scan statistics tend to detect the most likely cluster much larger than the true cluster by swallowing neighbouring regions with non-elevated risk. This paper proposes a new spatial scan statistic free from such an undesirable property by modifying the likelihood ratio so that it scans only the regions with elevated risk. Monte Carlo Simulation study shows that the proposed circular spatial scan statistic is shown to have better ability to identify the true cluster compared with Kulldorff's one in all the cluster models considered. The proposed circular spatial scan statisitc is illustrated with mortality data from cerebrovascular disease in Tokyo Metropolitan area, Japan.

*Key words*: Cluster detection; hot-spot cluster; likelihood ratio test; Monte Carlo testing; spatial epidemiology.

## 1. Introduction

Many different test statistics have been proposed for detecting disease clustering (Lawson *et al.*, 1999; Waller and Gotway, 2004; Kulldorff, 2006). Especially, the spatial scan statistic proposed by Kulldorff and Nagarwalla (1995) and Kulldorff (1997) has been applied to a wide variety of epidemiological studies and also to disease surveillance for the detection of disease clusters along with SaTScan Software (Kulldorff *et al.*, 2006a). The spatial scan statistic tries to identify the *most likely cluster* (MLC) defined as the set of connected regions that attains the maximum likelihood ratio. However, since it uses a circular window to scan the potential cluster areas, it has difficulty in correctly detecting actual non-circular clusters. To detect arbitrarily shaped clusters which cannot be detected by the circular spatial scan statistic, Duczmal and

Received June 2008. Revised July 2008. Accepted August 2008.

Assunção (2004), Patil and Taillie (2004), Tango and Takahashi (2005) and Assunção *et al.* (2006) have proposed different spatial scan statistics. It should be noted that all of these scan statistics are based on maximizing the likelihood ratio.

Tango (2000) showed an interesting example that Kulldorff's circular spatial scan statistic detected an unrealistically large MLC consisting of 70 regions, much larger than expected from an observed disease map, by absorbing neighbouring regions with non-elevated risk of disease occurrence in his simulated data. Furthermore, Tango and Takahashi (2005) have shown examples in which Duczmal and Assunção's procedure detected quite large and peculiar shaped MLC that had the largest likelihood ratio among the three different MLCs, identified by three different spatial scan statistics, Kulldorff's, Duczmal and Assunção's and Tango and Takahashi's. These results casted a doubt on the validity of the model selection based on maximizing the likelihood ratio.

In this paper, we shall propose a new spatial scan statistic free from such an undesirable property by modifying the likelihood ratio so that it scans only the regions with elevated risk. The performance of the circular spatial scan statistic with the modified likelihood ratio is compared with Kulldorff's original one via Monte Carlo Simulations. The proposed circular spatial scan statistic is illustrated with mortality data from cerebrovascular disease in the areas of Tokyo Metropolis and Kanagawa prefecture in Japan.

## 2. Motivating Example

As a motivating example, we shall introduce here a part of Tango and Takahashi's (2005) results of the application of three spatial scan statistics — Kulldorff's, Duczmal and Assunção's, and Tango and Takahashi's — to a simulated disease map in the areas of Tokyo Metropolis and Kanagawa prefecture in Japan wherein there are $m = 113$ regions that comprise wards, cities, and villages (Figure 1). The variability of regional populations is: 25 percentile $= 56,704$, median $= 142,320$ and 75 percentile $= 200,936$. On this map, they simulated a random sample of $n = 235$ cases by assuming the hot-spot cluster regions $\{14, 15, 26, 27\}$ in which each region's relative risk was set to constant $\theta = 3.0$ and the cases to be Poisson distributed. Under the null hypothesis of no clustering, the expected number of cases for each region was set proportional to the population (see equation (2)). For comparison purpose, they set the maximum number of regions for the MLC to be $K = 15$ and used 999 replications for the Monte Carlo hypothesis testing (see section 3 for details). The results are shown in Table 1 and are summarized as follows.

- Kulldorff's circular spatial scan statistic detected 2 regions $\{14, 15\}$ as the MLC with log likelihood ratio LLR= 20.1 and Monte Carlo $p$-value $p = 1/(999 + 1) = 0.001$, and the estimated relative risk $\hat{\theta} = 3.47$.
- Tango and Takahashi's flexible spatial scan statistic detected 5 regions $\{14, 15, 26, 27, 33\}$ as

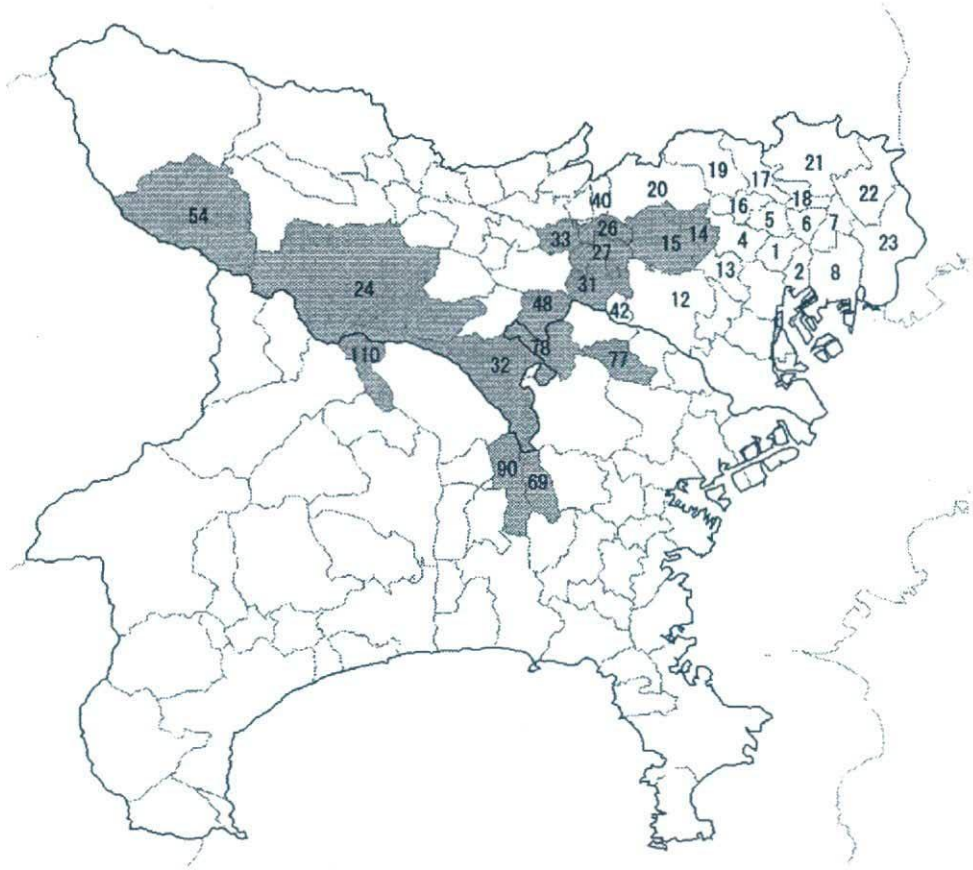


**Fig. 1.** An entire study population for simulation studies. The 113 regions that comprise wards, cities, and villages in the areas of Tokyo Metropolis and Kanagawa prefecture in Japan. The region number used in the text is shown. The shaded area was detected as the *most likely cluster* by Duczmal and Assunção's spatial scan statistic (see section 2).

the MLC with LLR= 29.7 and $p = 0.001$, and $\hat{\theta} = 3.41$.

- Duczmal and Assunção's spatial scan statistic detected 15 connected regions $\{14, 15, 24, 26, 27, 31, 32, 33, 48, 54, 69, 77, 78, 90, 110\}$ as the MLC (shaded area in Figure 1) with LLR= 31.8 and $p = 0.001$, and $\hat{\theta} = 2.41$.

All these spatial scan statistics rejected the null hypothesis of "$H_0$: there are no clusters," but detected different sets of connected regions as their MLC. In this example, Kulldorff's circular spatial scan statistic detected a small cluster consisting of only two regions out of four hot-spot cluster regions. In terms of maximizing the likelihood ratio, Duczmal and Assunção's spatial scan statistic is the best. However, their spatial scan statistic detected the MLC of a peculiar shape that was considerably larger than the true cluster, which includes eight regions $\{31, 48, 78, 32, 90, 69, 24, 110\}$ where each region's relative risk is not statistically significantly larger than 1 at 0.05 level. Table 1 shows the individual region's one-tailed *mid p-value*

**Table 1.** Regions detected as the most likely cluster by applying three procedures, Kulldorff's circular spatial scan, Tango and Takahashi's flexible spatial scan and Duczmal and Assuncao's spatial scan, to a simulated random sample $n = 235$ from the hot-spot cluster model. In the simulation, the true cluster is assumed to be $\{14, 15, 26, 27\}$ with constant relative risk $\theta = 3.0$. The maximum length (=number of regions) of cluster was set to be $K = 15$ (Tango and Takahashi, 2005).

| No. | region no. | observed no. cases | expected no. cases | relative risk (true) | One-tailed $p_i$ | Cumulative statistics LLR | O/E |
|---|---|---|---|---|---|---|---|
| 1 | 14 | 14 | 3.794 | 3.69(3) | 0.000027 | 8.3 | 3.69 |
| 2 | 15 | 21 | 6.283 | 3.34(3) | 0.000002 | 20.1 | 3.47 |
| Circular's MLC $= \{14, 15\}$, LLR $= 20.1$, $\hat{\theta} = 3.47$ | | | | | | | |
| 3 | 26 | 6 | 1.650 | 3.64(3) | 0.004 | 24.1 | 3.50 |
| 4 | 27 | 6 | 1.964 | 3.05(3) | 0.010 | 27.3 | 3.43 |
| 5 | 33 | 4 | 1.257 | 3.18(1) | 0.024 | 29.7 | 3.41 |
| Flexible's MLC $= \{14, 15, 26, 27, 33\}$, LLR $= 29.7$, $\hat{\theta} = 3.41$ | | | | | | | |
| 6 | 31 | 3 | 2.346 | 1.28(1) | 0.313 | 28.1 | 3.12 |
| 7 | 48 | 1 | 0.696 | 1.44(1) | 0.328 | 27.8 | 3.06 |
| 8 | 78 | 2 | 1.485 | 1.35(1) | 0.312 | 27.2 | 2.93 |
| 9 | 32 | 5 | 4.142 | 1.21(1) | 0.318 | 25.2 | 2.63 |
| 10 | 77 | 5 | 2.109 | 2.37(1) | 0.042 | 27.2 | 2.60 |
| 11 | 90 | 5 | 2.312 | 2.16(1) | 0.057 | 29.0 | 2.57 |
| 12 | 69 | 3 | 1.419 | 2.11(1) | 0.114 | 30.0 | 2.55 |
| 13 | 24 | 8 | 5.534 | 1.45(1) | 0.152 | 30.0 | 2.37 |
| 14 | 110 | 1 | 0.256 | 3.91(1) | 0.127 | 30.7 | 2.38 |
| 15 | 54 | 1 | 0.045 | 22.20(1) | 0.022 | 31.8 | 2.41 |
| Duczmal et al.'s MLC $= \{14, 15, 26, 27, 33, 31, \ldots, 54\}$, LLR $= 31.8$, $\hat{\theta} = 2.41$ | | | | | | | |

defined later in (7). This surprising result casts a doubt on the validity of the model selection based upon maximizing the likelihood ratio. Such a doubt can also be seen in Tango and Takahashi's simulation results of Kulldorff's circular spatial scan statistic that had non-negligible probabilities of detecting much longer clusters than the true cluster.

## 3. A New Spatial Scan Statistic

Consider the situation where an entire study area is divided into $m$ regions (for example, county, enumeration districts, etc.). The number of cases in the region $i$ is denoted by the random variable $N_i$ with observed value $n_i\,(i = 1, \ldots, m)$ and $n = n_1 + \cdots + n_m$. Under the null hypothesis $H_0$ of no clustering, the $N_i$ are independent Poisson variables such that

$$H_0 \colon E(N_i) = \xi_i,\ N_i \sim \mathrm{Pois}(\xi_i), \quad i = 1, \ldots, m \tag{1}$$

where $\mathrm{Pois}(\xi)$ denotes Poisson distribution with mean $\xi$ and the $\xi_i$ are the expected number of cases in the region $i$ under the null hypothesis. For the calculation of the expected number of cases adjusted for the potential confounders such as age, we can use an indirect standardization or a

Poisson mixed-effects regression model (Kulldorff *et al.*, 2006a). If we can ignore the confounders, the $\xi_i$ can be calculated as

$$\xi_i = n\frac{w_i}{\sum_{k=1}^{m} w_k}, \quad i = 1,\ldots,m \tag{2}$$

where $w_i$ denotes the population size in the region $i$. To specify the geographical position of each region, we will use the coordinates of the administrative population centroid.

Under this situation, Kulldorff's circular spatial scan statistic imposes a circular window $\mathbf{Z}$ on each centroid. For any of those centroids, the radius of the circle varies continuously from zero upwards until 50 percent of the population at risk is covered, which is the standard option for SaTScan. If the window contains the centroid of a region, then that whole region is included in the window. In total, a very large number of different but overlapping circular windows are created, each with a different location and size, and each being a potential cluster. Let $\mathbf{Z}_{ik}\,(k = 1,\ldots,K_i)$ denote the window composed by the $(k-1)$-nearest neighbours to region $i$. Then, all the windows to be scanned by the circular spatial scan statistic are included in the set

$$\mathcal{Z} = \{\mathbf{Z}_{ik} \mid 1 \le i \le m,\ 1 \le k \le K_i\}$$

Under the alternative hypothesis, there is at least one window $\mathbf{Z} \in \mathcal{Z}$ for which the underlying risk is higher inside the window when compared with outside. In other words, we are considering the following hypothesis testing:

$$\begin{aligned} H_0&: E(N(\mathbf{Z})) = \xi(\mathbf{Z}), \quad \text{for all } \mathbf{Z} \in \mathcal{Z} \\ H_1&: E(N(\mathbf{Z})) > \xi(\mathbf{Z}), \quad \text{for some } \mathbf{Z} \in \mathcal{Z} \end{aligned} \tag{3}$$

where $N()$ and $\xi()$ denote the random variable for the number of cases and the null expected number of cases within the specified window, respectively. For each window, it is possible to compute the likelihood to observe the observed number of cases within and outside the window, respectively. Under the assumption of Poisson distribution (1), Kulldorff's likelihood ratio test statistic is given by

$$\sup_{\mathbf{Z}\in\mathcal{Z}} \lambda_K(\mathbf{Z}) = \sup_{\mathbf{Z}\in\mathcal{Z}} \left(\frac{n(\mathbf{Z})}{\xi(\mathbf{Z})}\right)^{n(\mathbf{Z})} \left(\frac{n-n(\mathbf{Z})}{n-\xi(\mathbf{Z})}\right)^{n-n(\mathbf{Z})} I\left(\frac{n(\mathbf{Z})}{\xi(\mathbf{Z})} > \frac{n-n(\mathbf{Z})}{n-\xi(\mathbf{Z})}\right) \tag{4}$$

where $n()$ denotes the observed number of cases within the specified window and $I()$ is the indicator function. The window $\mathbf{Z}^*$ that attains the maximum likelihood ratio is defined as the *most likely cluster* (MLC). However, it seems something wrong to me that the likelihood ratio defined above does not take individual observed relative risk $n_i/\xi_i$ into account even if the MLC includes some regions with non-elevated risk, such as a region with $n_i/\xi_i \approx 1$. This property leads to the following proposition.

***Proposition***:

In the process of scanning the window based on $\sup_{\mathbf{Z}\in\mathcal{Z}} \lambda_K(\mathbf{Z})$, there is a possibility that there exists two disjoint windows $\mathbf{Z}_1$ and $\mathbf{Z}_2$ and several regions $\{i_1\},\ldots,\{i_r\}$ such that

$$\lambda_K(\{\mathbf{Z}_1,\mathbf{Z}_2,\{i_1\},\ldots,\{i_r\}\}) > \max\{\lambda_K(\mathbf{Z}_1),\ \lambda_K(\mathbf{Z}_2)\} \tag{5}$$

where

$$\frac{n(\mathbf{Z}_1)}{\xi(\mathbf{Z}_1)} > 1, \quad \frac{n(\mathbf{Z}_2)}{\xi(\mathbf{Z}_2)} > 1 \quad \text{and} \quad \frac{n_i}{\xi_i} \leq 1\ (i=1,\ldots,r)$$

For example, we can easily consider the following example:

***An example***: Suppose that $n = 200$ and two windows $\mathbf{Z}_1\,(n(\mathbf{Z}_1) = 30,\ \xi(\mathbf{Z}_1) = 12,\ \log\lambda_K(\mathbf{Z}_1) = 8.88)$ and $\mathbf{Z}_2\,(n(\mathbf{Z}_2) = 29,\ \xi(\mathbf{Z}_2) = 13,\ \log\lambda_K(\mathbf{Z}_2) = 7.97)$ were created in the process of scanning windows. Let 5-nearest neighbours to $\mathbf{Z}_1$ be $\{i_1\},\{i_2\},\ldots,\{i_4\}$, $\mathbf{Z}_2$ where four regions have non-elevated risk such as $(n_{i_1} = 4,\ \xi_{i_1} = 5)$, $(n_{i_2} = 6,\ \xi_{i_2} = 6)$, $(n_{i_3} = 0,\ \xi_{i_3} = 3)$, $(n_{i_4} = 8,\ \xi_{i_4} = 9)$. In this case, we have

$$\log\lambda_K(\{\mathbf{Z}_1,\mathbf{Z}_2,\{i_1\},\ldots,\{i_4\}\}) = 9.58$$

which satisfies equation (5).

The above proposition and example mean that if we allow any window and/or region to be a candidate for the MLC it causes the possibility of detecting an unrealistically large MLC by swallowing up neighboring regions with non-significantly elevated risk due to random fluctuation or with non-elevated risk as is shown in section 2. Therefore, to avoid such undesirable phenomena, we propose the following restricted likelihood ratio test statistic by taking individual region's risk into account:

$$\sup_{\mathbf{Z}\in\mathcal{Z}} \lambda_T(\mathbf{Z}) = \sup_{\mathbf{Z}\in\mathcal{Z}} \left(\frac{n(\mathbf{Z})}{\xi(\mathbf{Z})}\right)^{n(\mathbf{Z})} \left(\frac{n-n(\mathbf{Z})}{n-\xi(\mathbf{Z})}\right)^{n-n(\mathbf{Z})} I\left(\frac{n(\mathbf{Z})}{\xi(\mathbf{Z})} > \frac{n-n(\mathbf{Z})}{n-\xi(\mathbf{Z})}\right) \prod_{i\in\mathbf{Z}} I\,(p_i < \alpha_1) \tag{6}$$

where $p_i$ is the one-tailed $p$-value of the test for $H_0$: $E(N_i) = \xi_i$ given by the *mid-p value*

$$p_i = \Pr\{N_i \geq n_i + 1 \mid N_i \sim \text{Pois}(\xi_i)\} + \frac{1}{2}\Pr\{N_i = n_i \mid N_i \sim \text{Pois}(\xi_i)\} \tag{7}$$

and $\alpha_1$ is the pre-specified significance level for the individual region. The reason why the *mid-p value* was used is to adjust for conservatism of the ordinary definition of $p$-value for small $\xi_i$. In this formulation, we devised $I(p_i < \alpha_1)$ as a screening criterion and we do not mean that we are performing multiple hypothesis tests. Therefore, as in the case of the Kulldorff's circular spatial scan statistic, the restricted likelihood ratio test $\sup_{\mathbf{Z}\in\mathcal{Z}} \lambda_T(\mathbf{Z})$ of the nominal $\alpha_0$ level of 0.05, say, can be based on its distribution derived from a large number of Monte Carlo replications of the data set generated under the null hypothsis. Under this framework, the $p$-value is obtained

through Monte Carlo hypothesis testing (Dwass, 1957), by comparing the rank of the maximum likelihood from the real data set with the maximum likelihoods from the random data sets. If this rank is $R$, then $p = R/(1 + \#(\text{replications}))$.

Well, how is $\alpha_1$ chosen? If $\alpha_1$ is chosen too small then clusters might be missed or be too small, however, if chosen too large then it becomes equivalent to the Kulldorff's spatial scan statistic. So, we shall examine how sensitive the proposed method is to the selection of $\alpha_1$ and the optimal range of $\alpha_1$, by using five different values, 0.05, 0.10, 0.20, 0.30, 0.40, via Monte Carlo simulations in section 5, which might depend on both the cluster size and risk size.

It should be noted that the restricted likelihood ratio test statistic (6) is set to scan only for clusters with high relative risk. It also can be set to scan only for clusters with low relative risk by replacing the inequality ">" of the indicator function $I()$ which compares the observed relative risks within and outside the window $\mathbf{Z}$ with "<" and using the following *mid-p* value:

$$p_i = \Pr\{N_i \leq n_i - 1 \mid N_i \sim \text{Pois}(\xi_i)\} + \frac{1}{2}\Pr\{N_i = n_i \mid N_i \sim \text{Pois}(\xi_i)\}. \tag{8}$$

When we would like to scan for either high or low relative risk, we have only to delete the indicator function regarding the comparison of the observed relative risks and replace $\alpha_1$ with $\alpha_1/2$ in equation (6) using either *mid-p* value. Needless to say, maximizing the restricted likelihood ratio $\lambda_T(\mathbf{Z})$ can be applied not only to the circular spatial scan statistic but also to non-circular spatial scan statistics such as Duczmal and Assunção's (2004) and Tango and Takahashi's (2005).

## 4. Illustrations

As an illustration, we shall apply the proposed circular spatial scan statistic and Kulldorff's circular spatial scan statistic to the mortality data from cerebrovascular disease (female, 1993-1997) in the areas of Tokyo Metropolis and Kanagawa prefecture in Japan. Total observed number of deaths from female cerebrovascular disease for five years was 45,700 in this area. Regarding the restriction of the maximum length for the MLC, we shall select a standard option of SaTScan that the radius of the circle varies continuously from zero upwards until 50 percent of the population at risk is covered. $P$-value of the spatial scan statistics is calculated using 9999 replications for the Monte Carlo hypothesis testing. Significance levels considered are $\alpha_0 = 0.05$ and $\alpha_1 = 0.05, 0.10, 0.20, 0.30, 0.40$. Results are shown in Table 2 and summarized as follows: Irrespective of significance levels $\alpha_1$ chosen, the proposed circular spatial scan statistic detected the same MLC consisting of six regions $\{23, 22, 7, 8, 6, 18\}$ (these region numbers are shown in Figure 1) with $\log\lambda_T\,(=\log\lambda_K) = 126.6$, $\hat{\theta} = 1.23$, and $p = 1/(999+1) = 0.001$. All of these six regions within the MLC are shown to have highly significantly elevated risk. In contrast, Kulldorff's circular spatial scan statistic added six more regions $\{5, 1, 17, 21, 2, 16\}$ to the MLC detected by the proposed circular spatial scan statistic and finaly detected a larger MLC consisting of 12 regions with $\log\lambda_K = 140.6$ ($\log\lambda_T = 0$), $\hat{\theta} = 1.17$, and $p = 0.001$. However, three regions $\{5, 1, 2\}$ do not have significantly elevated risks. Especially, the region $\{5\}$, called

**Table 2.** The most likely clusters detected at $\alpha_0 = 0.05$ by the proposed circular spatial scan statistic and Kulldorff's circular spatial scan statistic in their application to the mortality data from cerebrovascular disease (female, 1993-1997) in the areas of Tokyo Metropolis and Kanagawa prefecture in Japan. The MLC detected by the proposed procedure was the same irrespective of values of $\alpha_1 = 0.05, 0.10, 0.20, 0.30, 0.40$.

| No. | region no. | observed no. cases | expected no. cases | relative risk | One-tailed $p_i$ |
|---|---|---|---|---|---|
| 1 | 23 | 1297 | 1072.3 | 1.21 | $1.5 \times 10^{-11}$ |
| 2 | 22 | 1266 | 1013.2 | 1.25 | $1.0 \times 10^{-14}$ |
| 3 | 18 | 738 | 522.7 | 1.41 | $< 1.0 \times 10^{-17}$ |
| 4 | 7 | 737 | 620.4 | 1.19 | $2.7 \times 10^{-6}$ |
| 5 | 8 | 896 | 780.6 | 1.15 | $2.7 \times 10^{-5}$ |
| 6 | 6 | 678 | 550.5 | 1.23 | $7.7 \times 10^{-8}$ |
| | | The proposed circular scan's MLC $= \{23, 22, 18, 7, 8, 6\}$ | | | |
| | | $\log \lambda_T = 126.6$, $\hat{\theta} = 1.23$, $p$-value $= 0.001$ | | | |
| 7 | 5 | 548 | 566.3 | 0.97 | 0.778 |
| 8 | 1 | 164 | 144.7 | 1.13 | 0.057 |
| 9 | 17 | 1110 | 999.3 | 1.11 | 0.00029 |
| 10 | 21 | 1530 | 1335.1 | 1.15 | $9.2 \times 10^{-8}$ |
| 11 | 2 | 267 | 251.3 | 1.06 | 0.161 |
| 12 | 16 | 798 | 743.4 | 1.07 | 0.024 |
| | | Kulldorff's circular scan's MLC $= \{23, 22, 18, 7, 8, 6, 5, 1, 17, 21, 2, 16\}$ | | | |
| | | $\log \lambda_K = 140.6$, $\hat{\theta} = 1.17$, $p$-value $= 0.001$ | | | |

"Bunkyo-ku," is well known as "healthy district" in this area and has a low relative risk of 0.97 and $p_5 = 0.778$ as expected. Therefore, it seems unacceptable to residents in "Bunkyo-ku" that their region is added to the MLC.

It should be noted that three regions $\{17, 21, 16\}$ have highly significant risk and are adjacent to the MLC detected by the proposed procedure. Therefore, the window $\{23, 22, 7, 8, 6, 18, 17, 21, 16\}$ could be a candidate for the MLC. In fact, its log likelihood ratio is $\log \lambda_T = 149.8$ which is larger than that of two MLCs. Needless to say, this non-circular window cannot be detected by circular spatial scan statistics and thus may be detected by such non-circular spatial scan statistic as that proposed by Duczmal and Assunção (2004) or Tango and Takahashi (2005) by applying the restricted likelihood ratio test statistic.

## 5. Power Comparisons

In this section, we shall compare the power of Kulldorff's circular spatial scan statistic with that of the proposed circular spatial scan statistic via Monte Carlo simulations at significance level $\alpha_0 = 0.05$ and examine the effect of the choice of $\alpha_1$ by using five different values $\alpha_1 = 0.05, 0.10, 0.20, 0.30, 0.40$. As an entire study population, we will use the area of Tokyo Metropolis and Kanagawa prefecture in Japan (Figure 1), described in section 2. In our simulation study, we consider two extremes regarding the sample size $n$: one assume rare disease with

total observed number of cases $n = 200$, a similar sample size used in section 2 and the other assumes non-rare disease with $n = 45,700$, the same $n$ for the cerebrovascular disease illustrated in section 4.

The same null hypothesis is used throughout, where the relative risk is set to one for each region and case locations are independent of each other. Although the $N_i$ are independent Poisson random variables, by conditioning on the total number of cases $N_+ = n$, the disease locations are the values of a random sample of size $n$ from a multinomial distribution with parameter $(\xi_1/n, \ldots, \xi_m/n)$. We generated 10,000 random data sets with $n$ cases and these are used to estimate the upper $100\alpha_0$ percent point for significance. Under each alternative hypothesis, we generated 1,000 random data sets with $n$ cases.

Alternative hypotheses $H_1$ considered here assume a single cluster $\mathbf{R} = \{i_1, \ldots, i_{s^*}\}$ with values of relative risk $\boldsymbol{\theta}_R = (\theta_{i_1}, \ldots, \theta_{i_{s^*}})$, i.e.,

$$H_1 : N_{i_k} \sim \mathrm{Pois}(\theta_{i_k}\xi_{i_k}), \quad k = 1, \ldots, s^* \tag{9}$$

where $s^*$ denote the size or length of the cluster assumed in the simulation. As cluster models, we considered here two types of clusters, namely, "clinal" and "hot-spot" clusters, defined by Wartenberg and Greenberg (1990). Clinal clusters have a monotone decrease in disease risk as distance from the point source increases. Hot-spot clusters are characterized by a constant elevated disease risk, i.e., $\theta_{i_1} = \cdots = \theta_{i_{s^*}} = \theta$. Under $H_1$, we generated a random sample $(n_1, \ldots, n_m)$ of size $n$ from a multinomial distribution with parameter $(q_1, \ldots, q_m)$ where

$$q_i = \frac{\pi_i w_i}{\sum_{k=1}^{m} \pi_k w_k} \tag{10}$$

where

$$\pi_i = \begin{cases} \theta_i & \text{if } i \in \mathbf{R} \\ 1, & \text{otherwise.} \end{cases}$$

In order to compare the performance of the spatial scan statistic based on Monte Carlo simulation, we shall use the bivariate power distribution $P(l, s)$ proposed by Tango and Takahashi (2005), which is classified according to the *length* $l$ of the significant MLC and the number $s$ of the assumed hot-spot regions included therein. It is estimated by

$$P(l, s) = \frac{\#\{\text{significant MLC has } \textit{length } l \text{ and includes } s \text{ true regions}\}}{\#\{\text{trials for each simulation}\}}, \tag{11}$$

where $1 \leq l$ and $0 \leq s \leq \min\{l, s^*\}$. Especially, we are interested in the power around the point $(l = s^*,\ s = s^*)$ and $P(s^*, s^*)$, the probability of exact detection. Then, the usual power is defined as the sum of $P(l, s)$:

$$P(+,+) = \sum_{l=1}^{l_{\max}} \sum_{s=0}^{\min\{l, s^*\}} P(l, s) = 1 - P(0, 0) \tag{12}$$

where $l_{\max}$ denotes the maximum *length* $l$ observed in the simulation and $P(0,0)$ denotes the probability that the spatial scan statistic cannot detect any clusters. However, when the support of the bivariate power distribution is widely scattered over the plane $(l,s)$, we do not think that we can use the usual power as the primary criterion to evaluate the performance because the performance of the spatial scan statistic is not only to reject the null hypothesis but also to identify the cluster accurately.

### 5.1 Case of Rare Disease

We examined several sets of cluster models with different relative risk $\boldsymbol{\theta}_R$ and cluster length $s^*$ and we shall report here the results of the following two hot-spot clusters and two clinal clusters since these models provided us with typical results.

1. Hot-spot cluster $\mathbf{A} = \{14, 15, 20\}$ with relative risk $\boldsymbol{\theta}_A = (3.0, 3.0, 3.0)$, $(s^* = 3)$.
2. Clinal cluster $\mathbf{B} = \{14, 15, 26, 27\}$ with relative risk $\boldsymbol{\theta}_B = (2.5, 3.0, 3.0, 2.5)$, $(s^* = 4)$
3. Hot-spot cluster $\mathbf{C} = \{1, 4, 5, 12, 13, 14, 15, 16, 19, 20\}$ with relative risk
   $\boldsymbol{\theta}_C = (2.0, 2.0, 2.0, 2.0, 2.0, 2.0, 2.0, 2.0, 2.0, 2.0)$, $(s^* = 10)$
4. Clinal cluster $\mathbf{D} = \{12, 14, 15, 20, 26, 27, 31, 33, 40, 42\}$ with relative risk
   $\boldsymbol{\theta}_D = (1.8, 1.8, 1.8, 2.2, 2.4, 2.4, 2.2, 2.2, 2.0, 1.8)$, $(s^* = 10)$

Two clusters **A** and **B** are examples of a very sharp increase in risk in a very small area in which the increase in each region within the cluster has more than 65% chance of being significant at $\alpha_1 = 0.05$ level. The clusters **C** and **D** are, on the other hand, examples of smaller increase in risk in a larger area consisting of $s^* = 10$ regions, in which the increase in each region within the cluster has less than 50% chance of being significant at $\alpha_1 = 0.05$ level. Regarding the shape of cluster, the clusters **A** and **C** are circular clusters that can be in the set of the circular windows and is expected to be identified exactly by the circular spatial scan statistic. The clusters **B** and **D** are non-circular clusters that are not in the set of the circular windows and thus cannot be identified exactly by the circular spatial scan statistic. The estimated bivariate power distribution $P(l,s) \times 1000$ is shown in Tables 3-6 for each of the three cluster models, respectively, in the form of cross table classified by $l$ ("*length*" in tables) and $s$ ("*include*" in tables).

Table 3 shows a good characteristic of the proposed circular spatial scan statistic. Namely, it could detect the hot-spot circular cluster **A** with length $s^* = 3$ considerably accurately with powers $P(3,3) = 0.834, 0.864, 0.767, 0.755, 0.748$ for $\alpha_1 = 0.05, 0.10, 0.20, 0.30, 0.40$, respectively. When we also evaluate the power of detecting the true cluster plus additional one region, its power was also high without reference to the value of $\alpha_1$, i.e., $P(3,3) + P(4,3) = 0.882, 0.976, 0.957, 0.918, 0.906$ for $\alpha_1 = 0.05, 0.10, 0.20, 0.30, 0.40$, respectively. The maximum length of the MLCs among all the results was only $l = 8$. On the other hand, Kulldorff's circular spatial scan statistic also had relatively high powers such as $P(3,3) = 0.672$ and $P(3,3) + P(4,3) = 0.819$. However, the estimated bivariate power distribution had a long tail to the right on the line $s = 3$ and the maximum length was 47. Usual power of the proposed circular spatial scan statistic was larger

**Table 3.** Estimated bivariate power distributions $P(l,s) \times 1000$ of Kulldorff's circular spatial scan statistic and the proposed circular spatial scan statistic for the hot-spot circular cluster $\mathbf{A} = \{14,15,20\}$ with relative risk $\boldsymbol{\theta}_A = (3.0,3.0,3.0)$ and $n = 200$. $\alpha_0 = 0.05$ and 1000 trials were carried out.

Kulldorff's circular scan

| Length $l$ | Include $s$ hot-spot regions | | | |
|---|---|---|---|---|
| | 0 | 1 | 2 | 3 |
| 1 | 1 | 0 | | |
| 2 | 0 | 0 | 0 | |
| 3 | 0 | 0 | 0 | 672 |
| 4 | 0 | 0 | 0 | 147 |
| 5 | 0 | 0 | 0 | 38 |
| 6 | 0 | 0 | 0 | 26 |
| 7 | 0 | 0 | 0 | 8 |
| 8 | 0 | 0 | 0 | 3 |
| 9 | 0 | 0 | 0 | 1 |
| 10 | 0 | 0 | 0 | 3 |
| 11 | 0 | 0 | 0 | 3 |
| 12 | 0 | 0 | 0 | 13 |
| 13 | 0 | 0 | 0 | 15 |
| 14 | 0 | 0 | 0 | 4 |
| 15 | 0 | 0 | 0 | 2 |
| 16-20 | 0 | 0 | 0 | 13 |
| 21-25 | 0 | 0 | 0 | 6 |
| 26-30 | 0 | 0 | 0 | 1 |
| 31-35 | 0 | 0 | 0 | 2 |
| 36-40 | 0 | 0 | 0 | 3 |
| 41-45 | 0 | 0 | 0 | 1 |
| 46-47 | 0 | 0 | 0 | 1 |
| Total | 1 | 0 | 0 | 962 |

usual power = 0.963

Proposed circular scan

| $\alpha_1$ | Length $l$ | Include $s$ hot-spot regions | | | | usual power |
|---|---|---|---|---|---|---|
| | | 0 | 1 | 2 | 3 | |
| 0.05 | 1 | 1 | 0 | | | 0.885 |
| | 2 | 1 | 0 | 0 | | |
| | 3 | 0 | 0 | 0 | 834 | |
| | 4 | 0 | 0 | 0 | 48 | |
| | 5 | 0 | 0 | 0 | 1 | |
| 0.10 | 1 | 1 | 0 | | | 0.984 |
| | 2 | 0 | 0 | 0 | | |
| | 3 | 1 | 0 | 0 | 864 | |
| | 4 | 0 | 0 | 0 | 112 | |
| | 5 | 0 | 0 | 0 | 5 | |
| | 6 | 0 | 0 | 0 | 1 | |
| 0.20 | 1 | 1 | 0 | | | 0.978 |
| | 2 | 0 | 0 | 0 | | |
| | 3 | 1 | 0 | 0 | 767 | |
| | 4 | 0 | 0 | 0 | 190 | |
| | 5 | 0 | 0 | 0 | 16 | |
| | 6 | 0 | 0 | 0 | 3 | |
| 0.30 | 1 | 1 | 0 | | | 0.978 |
| | 2 | 0 | 0 | 0 | | |
| | 3 | 1 | 0 | 0 | 755 | |
| | 4 | 0 | 0 | 0 | 163 | |
| | 5 | 0 | 0 | 0 | 42 | |
| | 6 | 0 | 0 | 0 | 16 | |
| 0.40 | 1 | 1 | 0 | | | 0.978 |
| | 2 | 0 | 0 | 0 | | |
| | 3 | 0 | 0 | 0 | 748 | |
| | 4 | 0 | 0 | 0 | 158 | |
| | 5 | 0 | 0 | 0 | 45 | |
| | 6 | 0 | 0 | 0 | 22 | |
| | 7-8 | 0 | 0 | 0 | 4 | |

than that of Kulldorff's circular spatial scan statistic except for the case of $\alpha_1 = 0.05$.

Table 4, on the other hand, shows that both Kulldorff's and the proposed circular spatial scan statistics had zero probability $P(4,4) = 0/1000$ for the exact detection since the clinal cluster **B** is non-circular. In this case, the support of the estimated bivariate power distribution of Kulldorff's circular spatial scan statistic was scattered over the plane $\{(l,s)\colon l \geq s,\ l = 1,2,\ldots,64,\ s = 0,2,3,4\}$ with the highest $P(2,2) = 0.311$. This type of simulation results are quite typical of

**Table 4.** Estimated bivariate power distributions $P(l,s) \times 1000$ of Kulldorff's circular spatial scan statistic and the proposed circular spatial scan statistic for the clinal non-circular cluster $\mathbf{B} = \{14, 15, 26, 27\}$ with relative risk $\boldsymbol{\theta}_B = (2.5, 3.0, 3.0, 2.5)$ and $n = 200$. $\alpha_0 = 0.05$ and 1000 trials were carried out.

Kulldorff's circular scan

| Length $l$ | Include $s$ clinal regions | | | | |
|---|---|---|---|---|---|
| | 0 | 1 | 2 | 3 | 4 |
| 1 | 5 | 0 | | | |
| 2 | 0 | 0 | 311 | | |
| 3 | 0 | 0 | 6 | 0 | |
| 4 | 0 | 0 | 5 | 0 | 0 |
| 5 | 0 | 0 | 2 | 0 | 0 |
| 6 | 0 | 0 | 1 | 0 | 0 |
| 7 | 0 | 0 | 1 | 15 | 0 |
| 8 | 0 | 0 | 5 | 7 | 18 |
| 9 | 0 | 0 | 1 | 1 | 9 |
| 10 | 0 | 0 | 2 | 15 | 5 |
| 11 | 0 | 0 | 1 | 1 | 3 |
| 12 | 0 | 0 | 0 | 3 | 32 |
| 13 | 0 | 0 | 1 | 2 | 35 |
| 14 | 0 | 0 | 0 | 4 | 16 |
| 15 | 0 | 0 | 0 | 1 | 2 |
| 16-20 | 0 | 0 | 2 | 2 | 53 |
| 21-25 | 0 | 0 | 0 | 0 | 43 |
| 26-30 | 0 | 0 | 0 | 0 | 16 |
| 31-35 | 0 | 0 | 0 | 0 | 15 |
| 36-40 | 0 | 0 | 0 | 0 | 5 |
| 41-45 | 0 | 0 | 0 | 0 | 5 |
| 46-50 | 0 | 0 | 0 | 0 | 7 |
| 51-55 | 0 | 0 | 0 | 1 | 1 |
| 56-60 | 0 | 0 | 0 | 0 | 0 |
| 61-64 | 0 | 0 | 0 | 1 | 1 |
| Total | 5 | 0 | 338 | 53 | 266 |

usual power = 0.662

Proposed circular scan

| $\alpha_1$ | Length $l$ | Include $s$ clinal regions | | | | | usual power |
|---|---|---|---|---|---|---|---|
| | | 0 | 1 | 2 | 3 | 4 | |
| 0.05 | 1 | 9 | 0 | | | | 0.748 |
| | 2 | 4 | 0 | 709 | | | |
| | 3 | 0 | 1 | 25 | 0 | | |
| 0.10 | 1 | 8 | 0 | | | | 0.754 |
| | 2 | 3 | 0 | 689 | | | |
| | 3 | 2 | 2 | 41 | 0 | | |
| | 4 | 1 | 0 | 8 | 0 | 0 | |
| | 5 | 1 | 0 | 0 | 0 | 0 | |
| 0.20 | 1 | 7 | 0 | | | | 0.685 |
| | 2 | 3 | 0 | 602 | | | |
| | 3 | 2 | 1 | 36 | 0 | | |
| | 4 | 1 | 1 | 26 | 0 | 0 | |
| | 5 | 1 | 0 | 3 | 0 | 0 | |
| | 6 | 0 | 0 | 0 | 2 | 0 | |
| 0.30 | 1 | 6 | 0 | | | | 0.689 |
| | 2 | 3 | 0 | 588 | | | |
| | 3 | 2 | 1 | 32 | 0 | | |
| | 4 | 1 | 1 | 30 | 0 | 0 | |
| | 5 | 1 | 0 | 4 | 0 | 0 | |
| | 6 | 0 | 0 | 5 | 11 | 0 | |
| | 7 | 0 | 0 | 0 | 0 | 0 | |
| | 8 | 0 | 1 | 1 | 1 | 2 | |
| 0.40 | 1 | 5 | 0 | | | | 0.693 |
| | 2 | 2 | 0 | 583 | | | |
| | 3 | 1 | 1 | 30 | 0 | | |
| | 4 | 1 | 1 | 29 | 0 | 0 | |
| | 5 | 1 | 0 | 7 | 0 | 0 | |
| | 6 | 0 | 0 | 4 | 0 | 0 | |
| | 7 | 0 | 0 | 1 | 3 | 0 | |
| | 8 | 0 | 0 | 2 | 4 | 2 | |
| | 9 | 0 | 0 | 0 | 2 | 2 | |
| | 10-12 | 0 | 0 | 0 | 2 | 0 | |

Kulldorff's circular spatial scan statistic when applied to non-circular clusters in our experience. In contrast, the proposed circular spatial scan statistic was shown to have higher powers for detecting a half of the true cluster, i.e., $P(2,2) + P(3,2) = 0.733, 0.730, 0.638, 0.620, 0.613$, for $\alpha_1 = 0.05, 0.10, 0.20, 0.30, 0.40$, respectively. Incidentally, the results that both spatial scan statistics had the highest detection probability at $(l,s) = (2,2)$ seem to be due to the geograph-

**Table 5.** Estimated bivariate power distributions $P(l,s) \times 1000$ of Kulldorff's circular spatial scan statistic for the hot-spot circular cluster $\mathbf{C} = \{1,4,5,12,13,14,15,16,19,20\}$ with relative risk $\boldsymbol{\theta}_C = (2.0,2.0,2.0,2.0,2.0,2.0,2.0,2.0,2.0,2.0)$ and $n = 200$. $\alpha_0 = 0.05$ and 1000 trials were carried out.

Kulldorff's circular scan

| Length $l$ | Include $s$ hot-spot regions | | | | | | | | | | |
|---|---|---|---|---|---|---|---|---|---|---|---|
| | 0 | 1 | 2 | 3 | 4 | 5 | 6 | 7 | 8 | 9 | 10 |
| 1 | 5 | 0 | | | | | | | | | |
| 2 | 0 | 0 | | | | | | | | | |
| 3 | 0 | 0 | 0 | 0 | | | | | | | |
| 4 | 0 | 0 | 0 | 0 | 0 | | | | | | |
| 5 | 0 | 0 | 0 | 0 | 0 | 0 | | | | | |
| 6 | 0 | 0 | 0 | 0 | 1 | 0 | 0 | | | | |
| 7 | 0 | 0 | 0 | 0 | 0 | 0 | 0 | 0 | | | |
| 8 | 0 | 0 | 0 | 0 | 0 | 0 | 0 | 0 | 0 | | |
| 9 | 0 | 0 | 0 | 0 | 0 | 0 | 0 | 0 | 0 | 0 | |
| 10 | 0 | 0 | 0 | 0 | 0 | 0 | 0 | 0 | 0 | 0 | 323 |
| 11 | 0 | 0 | 0 | 0 | 0 | 0 | 0 | 0 | 9 | 0 | 56 |
| 12 | 0 | 0 | 0 | 0 | 0 | 0 | 0 | 0 | 12 | 0 | 23 |
| 13 | 0 | 0 | 0 | 0 | 0 | 0 | 0 | 0 | 5 | 4 | 97 |
| 14 | 0 | 0 | 0 | 0 | 0 | 0 | 0 | 0 | 5 | 1 | 16 |
| 15 | 0 | 0 | 0 | 0 | 0 | 0 | 0 | 0 | 0 | 3 | 32 |
| 16 | 0 | 0 | 0 | 0 | 0 | 0 | 0 | 0 | 0 | 5 | 19 |
| 17 | 0 | 0 | 0 | 0 | 0 | 0 | 0 | 0 | 0 | 1 | 28 |
| 18 | 0 | 0 | 0 | 0 | 0 | 0 | 0 | 0 | 0 | 0 | 28 |
| 19 | 0 | 0 | 0 | 0 | 0 | 0 | 0 | 0 | 0 | 0 | 12 |
| 20 | 0 | 0 | 0 | 0 | 0 | 0 | 0 | 0 | 0 | 0 | 9 |
| 21-25 | 0 | 0 | 0 | 0 | 0 | 0 | 0 | 0 | 0 | 0 | 38 |
| 26-30 | 0 | 0 | 0 | 0 | 0 | 0 | 0 | 0 | 13 | 0 | 21 |
| 31-35 | 0 | 0 | 0 | 0 | 0 | 0 | 0 | 0 | 4 | 0 | 11 |
| 36-40 | 0 | 0 | 0 | 0 | 0 | 0 | 0 | 0 | 1 | 6 | 8 |
| 41-45 | 0 | 0 | 0 | 0 | 0 | 0 | 0 | 0 | 0 | 0 | 5 |
| 46-50 | 0 | 0 | 0 | 0 | 0 | 0 | 0 | 0 | 1 | 0 | 4 |
| 51 | 0 | 0 | 0 | 0 | 0 | 0 | 0 | 0 | 0 | 0 | 1 |
| Total | 5 | 0 | 0 | 0 | 1 | 0 | 0 | 0 | 50 | 20 | 731 |

usual power = 0.807

ical configulation of the non-circular cluster **B**. In this case, the proposed circular spatial scan statistic had larger usual powers than Kulldorff's circular spatial scan statistic without reference to the value of $\alpha_1$. Judging from the results shown in Tables 3-4, the result with $\alpha_1 = 0.10$ could be the best, however, the results with $\alpha_1 = 0.20 \sim 0.40$ were also shown to be better than Kulldorff's results.

Tables 5-6 show the results for the hot-spot circular cluster **C** where the affected area of regions is larger and the relative risk is smaller. In this instance, Kulldorff's circular spatial scan statistic was expected to detect changes in larger area that may not be obvious from each region individually and had surely high usual power 0.807 with the exact detection probability

**Table 6.** Estimated bivariate power distributions $P(l,s) \times 1000$ of the proposed circular spatial scan statistic for the hot-spot circular cluster $\mathbf{C} = \{1,4,5,12,13,14,15,16,19,20\}$ with relative risk $\boldsymbol{\theta}_C = (2.0,2.0,2.0,2.0,2.0,2.0,2.0,2.0,2.0,2.0)$ and $n = 200$. $\alpha_0 = 0.05$ and 1000 trials were carried out.

Proposed circular scan

| $\alpha_1$ | Length $l$ | Include $s$ hot-spot regions | | | | | | | | | | | usual power |
|---|---|---|---|---|---|---|---|---|---|---|---|---|---|
| | | 0 | 1 | 2 | 3 | 4 | 5 | 6 | 7 | 8 | 9 | 10 | |
| 0.05 | 1 | 10 | 0 | | | | | | | | | | 0.019 |
| | 2 | 6 | 0 | 0 | | | | | | | | | |
| | 3 | 1 | 0 | 0 | 0 | | | | | | | | |
| | 4 | 0 | 0 | 0 | 0 | 2 | | | | | | | |
| 0.10 | 1 | 8 | 0 | | | | | | | | | | 0.161 |
| | 2 | 7 | 0 | 0 | | | | | | | | | |
| | 3 | 2 | 0 | 0 | 0 | | | | | | | | |
| | 4 | 0 | 0 | 0 | 0 | 110 | | | | | | | |
| | 5 | 0 | 0 | 0 | 0 | 0 | 33 | | | | | | |
| | 6 | 0 | 0 | 0 | 0 | 0 | 1 | 0 | | | | | |
| 0.20 | 1-4 | 12 | 0 | 0 | 0 | 0 | | | | | | | 0.548 |
| | 5 | 0 | 0 | 0 | 0 | 0 | 403 | | | | | | |
| | 6 | 0 | 0 | 0 | 0 | 0 | 58 | 0 | | | | | |
| | 7 | 0 | 0 | 0 | 0 | 0 | 0 | 3 | 0 | | | | |
| | 8 | 0 | 0 | 0 | 0 | 0 | 0 | 0 | 0 | 0 | | | |
| | 9 | 0 | 0 | 0 | 0 | 0 | 0 | 0 | 0 | 0 | 71 | | |
| | 10-12 | 0 | 0 | 0 | 0 | 0 | 0 | 0 | 0 | 0 | 1 | 0 | |
| 0.30 | 1-5 | 9 | 0 | 0 | 0 | 0 | 0 | | | | | | 0.741 |
| | 6 | 0 | 0 | 0 | 0 | 1 | 0 | 0 | | | | | |
| | 7 | 0 | 0 | 0 | 0 | 0 | 0 | 3 | 0 | | | | |
| | 8 | 0 | 0 | 0 | 0 | 0 | 0 | 0 | 0 | 138 | | | |
| | 9 | 0 | 0 | 0 | 0 | 0 | 0 | 0 | 2 | 0 | 575 | | |
| | 10 | 0 | 0 | 0 | 0 | 0 | 0 | 0 | 1 | 0 | 0 | 0 | |
| | 11-12 | 0 | 0 | 0 | 0 | 0 | 0 | 0 | 0 | 9 | 3 | 0 | |
| 0.40 | 1-5 | 9 | 0 | 0 | 0 | 0 | 0 | | | | | | 0.744 |
| | 6 | 0 | 0 | 0 | 0 | 1 | 0 | 0 | | | | | |
| | 7 | 0 | 0 | 0 | 0 | 0 | 0 | 2 | 0 | | | | |
| | 8 | 0 | 0 | 0 | 0 | 0 | 0 | 0 | 0 | 135 | | | |
| | 9 | 0 | 0 | 0 | 0 | 0 | 0 | 0 | 6 | 0 | 568 | | |
| | 10 | 0 | 0 | 0 | 0 | 0 | 0 | 0 | 1 | 0 | 0 | 0 | |
| | 11 | 0 | 0 | 0 | 0 | 0 | 0 | 0 | 0 | 8 | 0 | 0 | |
| | 12 | 0 | 0 | 0 | 0 | 0 | 0 | 0 | 0 | 4 | 7 | 0 | |
| | 13-14 | 0 | 0 | 0 | 0 | 0 | 0 | 0 | 0 | 3 | 0 | 0 | |

$P(10,10) = 0.323$. However, the support of the estimated bivariate power distribution was again scattered over the broad area on the plane $\{(l,s)\colon l \geq s,\ l = 1,2,\ldots,51,\ s = 0,4,8,9,10\}$ by swallowing up many additional regions. In contrast, Table 6 shows that the support of the proposed circular spatial scan statistic was distributed in a relatively confined area on the plane $(l,s)$. However, the results with $\alpha_1 = 0.05$ and 0.10 were miserable, i.e., their usual power was quite low 0.039 and 0.161, respectively. As the value of $\alpha_1$ increases, the usual power increased to

0.548, 0.741 and 0.744 for $\alpha_1 = 0.20, 0.30$ and $0.40$, respectively. Although the probability of detecting the cluster exactly was zero without reference to the value of $\alpha_1$ chosen, the proposed circular spatial scan statistic was shown to have high probability of pinpointing eight or nine regions out of $s^* = 10$ regions, i.e., $P(8,8) + P(9,9) = 0.713, 0.703$ for $\alpha_1 = 0.30, 0.40$, respectively.

Tables 7-8 shows the results for the clinal non-circular cluster **D** where the affected area of regions is larger and the relative risk is smaller. Due to the non-circular shape, 1) both Kulldorff's and the proposed circular spatial scan statistic had zero probability of detecting the

**Table 7.** Estimated bivariate power distributions $P(l,s) \times 1000$ of Kulldorff's circular spatial scan statistic for the clinal non-circular cluster $\mathbf{D} = \{12, 14, 15, 20, 26, 27, 31, 33, 40, 42\}$ with relative risk $\boldsymbol{\theta}_D = (1.8, 1.8, 1.8, 2.2, 2.4, 2.4, 2.2, 2.2, 2.0, 1.8)$ and $n = 200$. $\alpha_0 = 0.05$ and 1000 trials were carried out.

Kulldorff's circular scan

| Length $l$ | Include $s$ clinal regions | | | | | | | | | | |
|---|---|---|---|---|---|---|---|---|---|---|---|
| | 0 | 1 | 2 | 3 | 4 | 5 | 6 | 7 | 8 | 9 | 10 |
| 1 | 3 | 0 | | | | | | | | | |
| 2 | 0 | 0 | 0 | | | | | | | | |
| 3 | 0 | 0 | 0 | 0 | | | | | | | |
| 4 | 0 | 0 | 0 | 0 | 24 | | | | | | |
| 5 | 0 | 0 | 0 | 0 | 0 | 0 | | | | | |
| 6 | 0 | 0 | 0 | 0 | 0 | 12 | 0 | | | | |
| 7 | 0 | 0 | 0 | 0 | 0 | 0 | 0 | 0 | | | |
| 8 | 0 | 0 | 0 | 0 | 0 | 0 | 29 | 0 | 0 | | |
| 9 | 0 | 0 | 0 | 0 | 0 | 0 | 0 | 0 | 0 | 0 | |
| 10 | 0 | 0 | 0 | 0 | 0 | 0 | 0 | 32 | 0 | 0 | 0 |
| 11 | 0 | 0 | 0 | 0 | 0 | 0 | 0 | 0 | 0 | 0 | 0 |
| 12 | 0 | 0 | 0 | 0 | 0 | 0 | 0 | 0 | 6 | 0 | 0 |
| 13 | 0 | 0 | 0 | 0 | 0 | 0 | 0 | 0 | 0 | 1 | 0 |
| 14 | 0 | 0 | 0 | 0 | 0 | 0 | 0 | 1 | 0 | 0 | 0 |
| 15 | 0 | 0 | 0 | 0 | 0 | 0 | 0 | 0 | 0 | 13 | 0 |
| 16 | 0 | 0 | 0 | 0 | 0 | 0 | 0 | 2 | 0 | 7 | 0 |
| 17 | 0 | 0 | 0 | 0 | 0 | 0 | 0 | 6 | 0 | 4 | 0 |
| 18 | 0 | 0 | 0 | 0 | 0 | 0 | 0 | 1 | 0 | 6 | 40 |
| 19 | 0 | 0 | 0 | 0 | 0 | 0 | 0 | 3 | 0 | 1 | 90 |
| 20 | 0 | 0 | 0 | 0 | 0 | 0 | 0 | 0 | 1 | 1 | 41 |
| 21-25 | 0 | 0 | 0 | 0 | 0 | 0 | 0 | 2 | 7 | 1 | 147 |
| 26-30 | 0 | 0 | 0 | 0 | 0 | 0 | 1 | 1 | 0 | 4 | 63 |
| 31-35 | 0 | 0 | 0 | 0 | 0 | 0 | 0 | 1 | 0 | 3 | 46 |
| 36-40 | 0 | 0 | 0 | 0 | 0 | 0 | 0 | 0 | 1 | 1 | 28 |
| 41-45 | 0 | 0 | 0 | 0 | 0 | 0 | 1 | 0 | 0 | 0 | 7 |
| 46-50 | 0 | 0 | 0 | 0 | 0 | 0 | 0 | 0 | 0 | 0 | 7 |
| 51-55 | 0 | 0 | 0 | 0 | 0 | 0 | 0 | 0 | 0 | 0 | 6 |
| 56-60 | 0 | 0 | 0 | 0 | 0 | 0 | 0 | 0 | 0 | 0 | 2 |
| 61-62 | 0 | 0 | 0 | 0 | 0 | 0 | 0 | 0 | 0 | 0 | 3 |
| Total | 3 | 0 | 0 | 0 | 24 | 12 | 31 | 49 | 15 | 42 | 480 |

usual power = 0.656